JOURNAL OF SOLID STATE CHEMISTRY 39, 368–376 (1981)

Studies of Zinc–Chromium Hydroxy Salts. I. Thermal Decomposition of $[Zn_2Cr(OH)_6]X \cdot nH_2O$, Where $X^- = F^-, Cl^-, Br^-, I^-, \frac{1}{2}CO_3^{2-}$, and NO_3^-.

MISRI LAL AND ARTHUR T. HOWE*

Department of Inorganic and Structural Chemistry, University of Leeds, Leeds LS2 9JT, England

Received March 2, 1981; in final form May 18, 1981

We have characterized the layered anion exchange compounds $[Zn_2Cr(OH)_6]X \cdot nH_2O$, where $X^- = F^-, Cl^-, Br^-, I^-, \frac{1}{2}CO_3^{2-}$, and NO_3^-, and studied their thermal decomposition. The precipitated particles were less than a few hundred angstroms in size, and could not be easily aged. Upon heating, a considerable amount of surface water, up to $n = 1$ in the formula, was initially lost, followed by the ill-defined stages represented by loss of water of hydration ($n \leq 2$), first stage of dehydroxylation, loss of X (over temperature ranges between 200 and 500°C) and final dehydroxylation (up to 700°C). Interest in such possible mixed $O^{2-}/OH^-/X^-$ decomposition intermediates as ionic conductors is discussed.

Introduction

Metal oxyhydroxides are of interest from the point of view of ionic conduction, since the presence of O^{2-}/OH^- pairs and possibly anion vacancies may favor proton or oxide ion conductivity, respectively. However, conduction studies of such oxyhydroxides as AlOOH (boehmite) (*1*, *2*), $Mg(OH)_{2-2x}O_x$ (*3*), and FeOOH (*4*) have revealed only poor conduction properties. Oxyhydroxides are usually prepared by controlled thermal decomposition of the parent hydroxide, and the recently reported (*5*) new hydroxide series $[Zn_2Cr(OH)_6]X \cdot nH_2O$, where X^- is an anion, aroused our interest as a possible precursor to oxyhydroxides which might also contain other anions such as halides. The presence of halide ions, for example, in addition to O^{2-} and OH^- ions, may perturb the local site energies in a way which may enhance the ionic conductivity. We therefore undertook a thermal investigation of the compounds, supported by a chemical and structural study, to ascertain whether stable intermediates could be produced, and we report our results here in Part I.

The parent compounds $[Zn_2Cr(OH)_6]X \cdot nH_2O$, even before decomposition, show unusual properties, such as anion exchange (*5*), and proton conductivity in the case of pressed pellets of the double hydroxide $[Zn_2Cr(OH)_6]OH \cdot \sim 2H_2O$ (*6*). We have also studied the conduction properties of the X^- ions in the hydroxy salts, and report this investigation in Part II (*7*), for which the characterization of the compounds described here in Part I forms an essential basis.

The series $[Zn_2Cr(OH)_6]X \cdot nH_2O$ possess positively charged layers having the brucite, $Mg(OH)_2$-type structure and represented by $[Zn_2Cr(OH)_6]^+$, in which the cations occupy, in an ordered fashion, the

* Present address: Amoco Research Center, PO Box 400, Naperville, Ill. 60566.

0022-4596/81/120368-09$02.00/0

octahedral sites between the two sheets of close-packed OH^- ions (*5*). The brucite-type layers are separated by interlayers containing the anions X^-, and water molecules.

Hydroxides having the same double-layer structural type as the zinc–chromium hydroxy salts were first identified by Feitknecht (*8*), and exist for a variety of metals with most anions, as reviewed by Allmann (*9*). In general, the ratio of trivalent to divalent metal can vary, as indicated by the formula $[M(II)_{1-x}M(III)_x(OH)_2]^{x+}[xX \cdot nH_2O]^{x-}$, where $M(II)$ can be Ca, Mn, Fe, Co, Ni, Zn, or Cd, and $M(III)$ can be Al, Cr, Mn, Fe, Co, Ni, or Ga. The minerals pyroaurite and sjögrenite belong to this class (*9*). Cation ordering can be detected by a change in the unit cell dimensions, and only the Zn–Cr (*5*) and the Ca–Al, Ca–Fe, Ca–Cr, and Ca–Ga compounds (*9*) show cation order. $[Ca_2Al(OH)_6]OH \cdot nH_2O$ occurs in cement (*10*), and the structure is distorted to give sevenfold coordination around the Ca^{2+} ions (*11*). The diffraction data indicate disorder in the OH^-/H_2O interlayers (*11*).

The thermal decomposition of $[Mg_4Al_2(OH)_{12}]CO_3 \cdot 3H_2O$ (*12*), related compounds (*13, 14*), Mg–Al double hydroxides (*15*), and $[Ca_2Al(OH)_6]OH \cdot 3H_2O$ (*16*) occur in two or three stages to finally produce the metal oxides at 500 to 600°C. Only the Ca–Al salt gives a well-defined intermediate product (*16*). Little is known of the decomposition behavior of other salts in this class.

Experimental

The samples were prepared following the method of Boehm *et al.* (*5*). To a slurry of 45 g ZnO and a little water was added 150 ml of 1 *M* $CrCl_3$ solution and 50 ml water to bring the pH to between 3 and 4, and the mixture was stirred for 5 hr at 60°C, after which time the solution had decolorized and the pH was 5. After decantation, a further 150 ml of 1 *M* $CrCl_3$ solution, bringing the total Zn/Cr ratio to 2, was added and the pH brought to between 3 and 4, and the mixture stirred for 5 hr at 60°C. The light purple-colored chloride was collected from the clear solution, and X-ray analysis showed no trace of other phases. The Zn/Cr ratio used in the preparation could be varied over a considerable range without a change in the X-ray pattern.

The other salts were prepared by twice exchanging 0.35 g of the chloride with 30 ml of 1 *M* solution of the appropriate sodium salt (a 30-fold excess) for 15 hr each at 60°C. The products were washed by repeatedly stirring with distilled water followed by centrifuging, or were boiled with a large quantity of distilled water which was then decanted and centrifuged off. The final solution pH's were typically between 5 and 7.

The samples were found to have water contents which varied with ambient conditions, a feature which was investigated by means of thermogravimetric analysis (TGA). Chemical analyses were therefore performed on samples equilibrated at an ambient temperature of 17°C. Chemical analysis of the chloride salt, using atomic absorption for Zn and Cr, and volumetric analysis for chloride, gave the elements present in the atomic ratios 2.00/1.04/1.02 respectively and, together with the hydrogen content obtained from a C–H–N analyzer, substantiate the composition as $[Zn_2Cr(OH)_6]Cl \cdot \sim 2H_2O$, as previously formulated (*5*).

Chloride analyses of each of the exchanged salts, apart from the bromide, for which an analysis could not be conveniently done, indicated greater than 98% conversion, which was undoubtedly aided by the higher exchange temperature of 60°C which was used compared to Boehm's conditions (*5*), under which sometimes only partial exchange was observed. The Zn/Cr ratios found in the exchanged salts were all

equal to 2 within the experimental errors. Reaction of the hydroxides with atmospheric CO_2 was found to be indetectable, as judged from C–H–N analyses, after heating selected samples in air at 50°C for 3 days. The formulations of the compounds with $X^- = \frac{1}{2}CO_3^{2-}$ and NO_3^- were confirmed by carbon and nitrogen analyses, respectively.

X-Ray parameters were obtained using Cr radiation and a Philips 1050/25 powder diffractometer fitted with a hot stage. The electron micrographs were obtained using a Cambridge Stereoscan 150 Mk 2 microscope. TGA and simultaneous differential thermal analysis (DTA) were performed on a Stanton Redcroft STA 780 microbalance instrument, using samples of about 20 mg with the thermal capacity reference pan empty to avoid possible degassing of the Al_2O_3 powder usually used. Laboratory air was passed over the samples at 50 ml min^{-1}, and the heating rate was 1° min^{-1}. The weights were corrected for the small effect of the gas flow as a function of temperature.

Results and Discussion

Structural Aspects

The X-ray peaks from the Zn–Cr salts were generally all quite broad, and in agreement with Boehm *et al.* (*5*), we also found that the (*hk*) reflections were broader than the (*l*) reflections. The reflections were consistent with a cation-ordered hexagonal unit cell with $a \approx 5.4$ Å for all compounds and $c \approx 7$–9 Å. The basal spacings are given in Table I, and are in satisfactory agreement with those of Boehm *et al.* (*5*).

An electron micrograph of the chloride is shown in Fig. 1, and clearly shows the typical presence of aggregates of 0.5 to 5 μm in size, comprising of intergrowths of many ill-defined smaller needles or plates of the order of 500 Å in thickness observed in both the initial chloride and the exchanged compounds. An extensive search of many samples did not show any evidence of discreet needles, and the needle shapes evident in the micrograph are interpreted as being plates end-on. Some larger plates, confirming this morphology, are clearly visible. The aggregates contrast with the published micrographs of the analogous Mg–Al double hydroxide (*17*), which show particles covering a similar size range, but which were hexagonal platelets with well-defined sharp edges. Judging from the sharp edges we observed from a crystalline control sample observed in the microscope under the same conditions as the Zn–Cr

TABLE I

BASAL SPACINGS *d*, ESTIMATED THICKNESSES *t*, AND WATER CONTENTS *n* AT 17°C OF $[Zn_2Cr(OH)_6]X \cdot nH_2O$

	d			
X^-	this work (±0.1 Å)	Ref. (*5*) (Å)	*t* (±20 Å)	*n*(±0.1)
F^-	7.48	7.51	105	2.7
Cl^-	7.77	7.73	110	2.9
Br^-	7.86	7.85	160	1.7
I^-	8.23	8.40	100	2.3
NO_3^-	8.75	8.88	130	3.0
$\frac{1}{2}CO_3^{2-}$	7.60	—	86	1.6

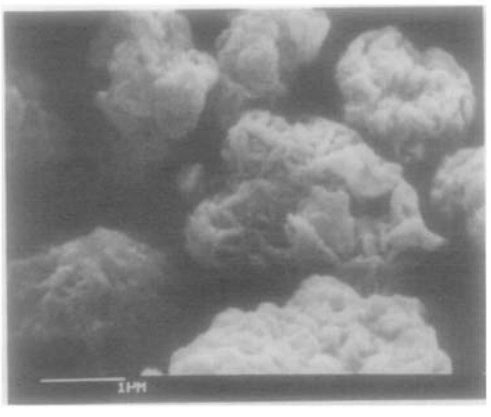

FIG. 1. Electron micrograph of the chloride salt.

salts, we estimate that the true size of the fundamental particles may be even smaller than the apparent size, due to the visible small shapes being composed of several smaller particles, of possible dimensions of several hundred angstroms each.

In agreement with Boehm *et al.* (*5*), we also found that the X-ray peaks did not become sharper upon boiling the samples in water. Furthermore, the electron micrographs of the exchanged materials, which had been further heated in solution at 60°C for a total of 30 hr, were not noticeably different from those of the original chloride. It would therefore appear that the small crystallites cannot be readily aged.

The observed breadth of the X-ray peaks (0.5 to 1°) is also well accounted for on the basis of very small particles. On this assumption, the thicknesses of the particles in the direction of the *c* axis have been calculated from the widths of the (001) reflections (*18*). The values fall between 86 to 160 Å, and are given in Table 1. Bearing in mind that possible stacking disorder among the layers may also contribute to the broadening of the X-ray reflections, the microscopic and X-ray techniques are in agreement in establishing very small-sized particles. The observed broadening of the (*hk*) reflections relative to the (*l*) reflections is a characteristic of the double salts, and is ascribed to turbostratic perturbation of the layers, to produce layer twisting and rippling (*19*).

Thermal Decomposition

Figure 2 shows the TGA and DTA curves for the compounds up to 800°C. There were no further weight changes between 800 and 1000°C, and the final products were assumed to be ZnO and Cr_2O_3 or reaction products of these oxides to give, for instance, spinel-type phases.

A cursory inspection of the curves shows the general absence of well-defined inter-

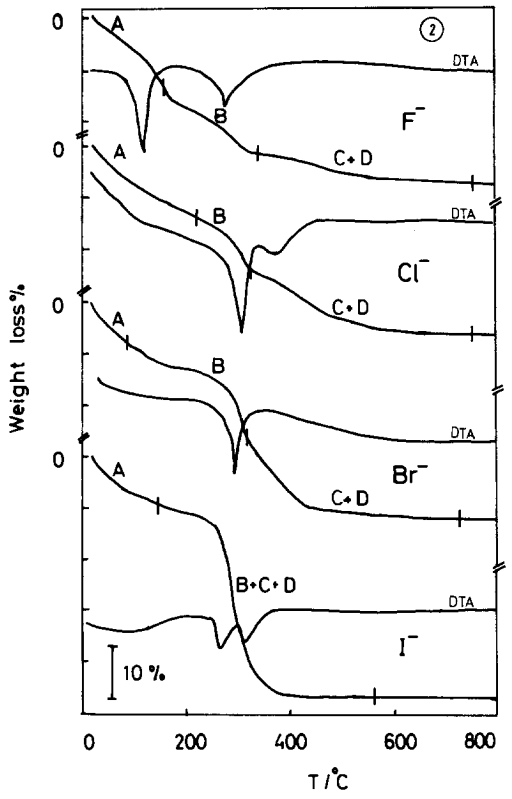

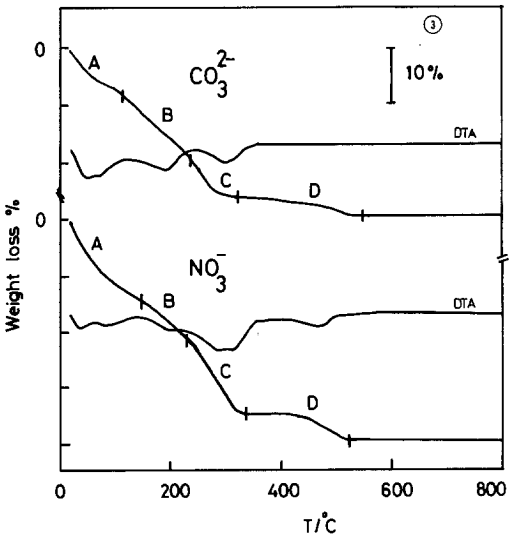

FIG. 2 and 3. Weight losses (scale as indicated) and thermal differentials (DTA, arbitrary scale) during decomposition of $[Zn_2Cr(OH)_6]X \cdot nH_2O$.

mediate weight plateaus. In view of the slow heating rate of 1° min^{-1} and relatively high gas flow of 50 ml min^{-1} it is likely that these are genuine broad transitions. Furthermore, for selected samples, when the heating was stopped and the sample held at a constant temperature, the weight remained almost constant, showing that the decomposition was not being suppressed by the experimental conditions or kinetics. Such broad transitions are also found in, for instance, the thermal decomposition of the Mg–Al analogs (*12–15*), as already mentioned, and of $Mg(OH)_2$ (*20*), which has the prototype brucite structure.

Let us first consider the thermal behavior, in relation to the structure, in the region of the initial weight losses, up to about 150°C.

Initial Weight Losses

A common feature of all of the TGA curves is the immediate weight loss observed upon heating above the ambient starting temperature of 17°C. Careful TGA runs on the chloride between 12 and 50°C did not reveal any plateaus in the thermogram. Furthermore, the weight increased upon increasing the water vapor pressure, and did not show any plateau before saturated conditions were reached. The variability of the water contents with conditions is thus a complicating feature in the interpretation of the ambient structure and dehydration behavior.

The water contents of the samples at 17°C were calculated from the TGA data taken at 17 and 1000°C, assuming the formula $[Zn_2Cr(OH)_6]X \cdot nH_2O$. The values of n obtained are shown in Table 1. General confirmation of the water contents was obtained from C–H–N analyses, although the calculated values of n were all slightly lower than those found from the TGA method. This is attributed to slight loss of water from the samples during the automated purge of dry He gas prior to the start of component monitoring by the detectors.

In the thermograms shown in Fig. 2 we have marked the weight losses corresponding to loss of n waters, as given in Table 1. It can be seen that the losses up to the corresponding temperatures of 100 to 250°C, as labeled A on the thermograms, can be satisfactorily assigned to water loss.

The spread in the observed values of n, from 3.0 down to 1.6, would normally be explained by proposing that the maximum hydrate was for $n = 3$, and that lower values of n were caused by partial dehydration. However, consideration of the structural model shows only three normal interlayer sites per formula. In the analogous compounds $[Ca_2Al(OH)_6]X \cdot 2H_2O$, where $X^- = Cl^-$, Br^-, or I^-, the two water molecules and the halide fill all the available normal interlayer sites (*21*). In view of the extremely small size of the particles in our case compared to the much larger-sized particles of the Ca–Al salts (*21*), it would seem likely that, for the Zn–Cr salts, additional water above $n = 2$ was surface water, probably stabilized in between the faces of adjacent crystallites.

Support for this view comes from the fact that pressed disks, held around the circumference by gluing them over a hole in a glass plate, cracked wide apart when heated to 50°C, due to a contraction of about 4%. However, the d spacing changed by less than 1% over the same conditions, showing that loss of water caused contraction between the particles, but not of the particles themselves, indicating loss of surface water.

We should mention that in the rather unique case of $[Ca_2Al(OH)_6]OH \cdot nH_2O$, higher hydrates, with $n = 3$ and 6, have been reported (*10*). The extra water molecules result, however, in lattice expansion, such that d is 10.6 Å for $n = 6$, 8.2 or 7.9 Å for the α and β forms respectively for $n = 3$, 7.4 Å for $n = 2$, and still 7.4 Å for $n = 0$

(*10*). Careful X-ray measurements on the Zn–Cr chloride revealed no change in the basal spacing, to within ±1% for moist powder, and powder in air at 20 and 90°C. Taking into consideration the smaller a unit cell dimension of the Zn–Cr salts (5.4 Å) compared to that of $[Ca_2Al(OH)_6]OH \cdot 3H_2O$ of 5.73 Å (*10*), and the larger radius of Cl^- compared to that of OH^-, the evidence would again suggest the absence of hydrates with n higher than 2 for the Zn–Cr chloride.

The observed loss of n waters in the continuous regions indicated as A in the thermograms is therefore attributed to loss of surface water together with intracrystalline waters of hydration, and overlaps with the first dehydroxylation stage, as will be discussed in the next section. The amount of surface water, up to one-third of the total, would appear to be quite large. However, considering the small particle size, this quantity would correspond approximately to three water layers on each crystallite surface. In addition, the loose agglomerates of particles evident in the micrograph shown in Fig. 1 could well contain internal water, even under equilibrium conditions. It is probable that the surface X^- ions "dissolve" in the surface water, since they would not be strongly bound to their normal sites on the surface. Such a donation would undoubtedly stabilize the surface water and account for its abundance. The implications of this feature for the room temperature ionic conductivities of the materials will be illustrated in Part II (*7*). We have left n in the formula to represent both surface and intracrystalline water, due to the difficulty in quantitatively differentiating between the two.

Further Stages of Decomposition of the Halides

On the basis of the results, the following decomposition scheme is proposed for the halides, in which the last two formulae represent only the overall compositions.

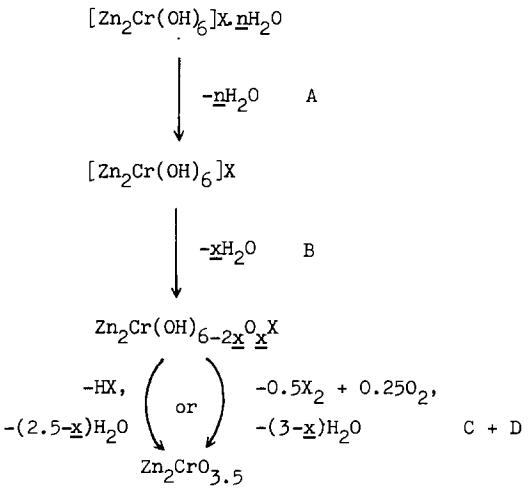

The regions A, B, C, and D are indicted in Fig. 2. Inspection of the thermograms shows that, after the initial water losses of region A, two further stages are discernible for all but the iodide, and we have labeled these B, and (C + D). The fact that stage (C + D) occurs at progressively lower temperatures for the fluoride, chloride, bromide, and iodide, while the temperature range of stage B remains reasonably constant suggests that stage (C + D) is associated with loss of halogen, and that stage B therefore represents dehydroxylation. This is confirmed for the fluoride since loss B exceeds the expected loss due to loss of HF or F_2. In the case of the chloride, loss B is larger, and does not allow such a distinction to be made. However, analysis of a chloride sample cooled from 350°C, just after region B, showed all the chloride still present, in confirmation of the proposed scheme.

Endotherms associated with stage B are seen to occur at 270, 300, 290, and 270°C for the F^-, Cl^-, Br^-, and I^- forms, respectively. The inflections at the ends of regions B for the fluoride and chloride correspond to $x = 2.5$ and 1.9, respectively. The X-ray

patterns of samples cooled from 350°C showed only very weak broad peaks indicative of poorly crystallized or finely divided material. In view of the thermal stability of CrOCl, which oxidizes to Cr_2O_3 in vacuum at 800°C (*22*), but which would oxidize at a lower temperature in air, as in this experiment, it is possible that after stage B the sample consists of CrOCl and a zinc oxyhydroxide. Although CrOF has not been previously reported, it may also possibly be present in the fluoride sample.

Turning to region (C + D), consideration of the weight losses shows that a distinction cannot be drawn between loss of halogen as HX, or as X_2 with associated reaction with O_2 of the air, and both of these reactions are indicated in the above scheme. Furthermore the weight losses in the case of the chloride exceed those due to either mode of loss of halogen, and therefore indicate that an overlapping second stage of dehydroxylation occurs, in this case corresponding to loss of 1.1 H_2O. Retention up to the region of 500 to 700°C of surface hydroxyl groups and isolated bulk hydroxyl groups kinetically hindered from reacting is a common feature of oxides produced by the decomposition of hydroxides (*23*). This effect might be expected to be pronounced in our high-surface-area samples. We have thus assigned loss of halogen to step C, and the second stage of dehydroxylation to the overlapping step D. Both these steps are shown in the above decomposition scheme. The final product, of overall composition $Zn_2CrO_{3.5}$, is probably a mixture of oxides, possibly together with the spinel phase $ZnCr_2O_4$.

Further Stages of Decomposition of the Carbonate and Nitrate

The data is presented in Fig. 3 and indicates the following decomposition sequence, where the last three formulae represent overall compositions only.

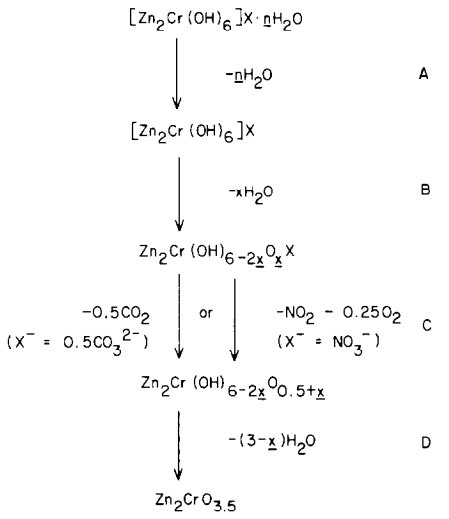

As with halides, the first step (A) is again loss of surface and hydration water. The markers in Fig. 3 at the ends of regions A correspond to loss of n waters, as given in Table I, and are seen to coincide with a trough between two endotherms, thus supporting the assignment.

Chemical analysis (C–H–N) of the products of decomposition at 350°C showed no significant proportions of C or N for the carbonate and nitrate respectively, indicating that region D is, like the halides, due to loss of water, which we assign to the second stage of dehydroxylation. From the weight losses over region D, values of x, referring to the above equations, were found to be 2.4 and 1.7 for the carbonate and nitrate, respectively.

Working backward from region D, it is found that loss of X prior to region D, that is in region C, as shown in the above scheme, coincides in the thermograms with temperatures of troughs between endotherms. This can be seen in Fig. 3 from the position of the markers between regions B and C. We therefore identify region C with loss of X, and region B therefore with the first stage of dehydroxylation, as shown in the above scheme.

In the case of the carbonate, the three

endotherms, which occur at 50, 200, and 300°C for reactions A, B, and C, respectively, indicate considerably lower decomposition temperatures than reported for the structurally related compounds manasseite and hydrotalcite, both of formula $[Mg_6Al_2(OH)_{16}]CO_3 \cdot 4H_2O$, for which crystalline water was not completely lost until 280°C, and dehydroxylation and decarbonation occurred, in an unassigned order, between 350 and 500°C (*14, 19*).

In the case of the nitrate, six endotherms are discernible, at 30 and 90°C (region A), 190°C (region B), 280, 320°C (region C) and 470°C (region D). Decomposition of the nitrate ion (region C) occurs within the range typical for transition metal nitrates of 200–350°C (*24*), and close to the decomposition temperature of pure $Zn(NO_3)_2$ of 350°C (*25*).

Conclusion

The study has revealed a variety of intermediate compositions, many of which may be present as mixed anion phases such as oxyhydroxy–halides/carbonates/nitrates, and at higher temperatures, just as oxyhydroxides. To the extent that the brucite structure type is retained during decomposition, the structure would possess anion vacancies arising from dehydroxylation, which may favor easy migration of any of the anions present (O^{2-}, OH^-, or X^-). In addition, the simultaneous presence of O^{2-} and OH^- in similar lattice sites is a favorable factor for proton migration. However, the ionic conductivities of none of the compounds, measured in a manner described elsewhere (*26*), was greater than 10^{-6} $ohm^{-1}\,cm^{-1}$ at 100°C, and did not rise above 10^{-5} $ohm^{-1}\,cm^{-1}$ up to 250°C (*27*). This is consistent with similarly low conductivities measured for other oxyhydroxides having the brucite type structure, namely, those derived from the thermal decomposition of $Mg(OH)_2$ and $Al(OH)_3$, and their mixtures and solid solutions with a wide range of cation and anion dopants (*27*), and would suggest that the factor most inhibiting ionic migration in these oxyhydroxides is the difficulty of jumping between sites rather than the availability of vacancies. However, the hydrated forms of the undecomposed Zn–Cr hydroxy salts exhibited some very interesting conduction features, which are reported in Part II (*7*), and the present study has established many of the structural and compositional aspects, in particular the nature of the hydration of the compounds, which will be drawn upon in the second part.

Acknowledgments

One of us, M.L., thanks the Science Research Council for a postdoctoral fellowship, and we thank Dr. M. G. Dobb of the Department of Textile Industries for obtaining the electron micrographs.

References

1. A. M. Arjona and J. J. Fripiat, *Trans. Faraday Soc.* **63**, 2936 (1967).
2. T. Takahashi, S. Tanase, O. Yamamoto, S. Yamauchi, and H. Kabeya, *Int. J. Hydrogen Energy* **4**, 327 (1979).
3. W. Gieseke, H. Nägerl, and F. Freund, *Naturwissenschaften* **10**, 493 (1970).
4. K. J. Gallagher and D. N. Phillips, *Trans. Faraday Soc.* **64**, 785 (1968).
5. H.-P. Boehm, J. Steinle, and C. Vieweger, *Angew. Chem.* **89**, 259 (1977); *Angew. Chem. Int. Ed. (English)* **16**, 265 (1977).
6. M. Lal and A. T. Howe, *J. Chem. Soc. Chem. Commun.*, 737 (1980).
7. M. Lal and A. T. Howe, *J. Solid State Chem.* **39**, 377 (1981).
8. W. Feitknecht, *Z. Angew. Chem.* **49**, 24 (1936).
9. v-R. Allmann, *Chimia* **24**, 99 (1970).
10. M. H. Roberts, *J. Appl. Chem.* **7**, 543 (1957).
11. S. J. Ahmed and H. F. W. Taylor, *Nature* **215**, 622 (1967).
12. G. Brown and M. C. Gastuche, *Clay Miner.* **7**, 193 (1967).
13. G. Mascolo and O. Marino, *Thermochim. Acta* **35**, 93 (1980).
14. G. J. Ross and H. Kodama, *Amer. Mineral.* **52**, 1036 (1967).

15. G. MASCOLO AND O. MARINO, *Mineralog. Mag.* **43,** 619 (1980).
16. F. G. BUTLER, L. S. DENT GLASSER, AND H. F. W. TAYLOR, *J. Amer. Ceram. Soc.* **42,** 121 (1959).
17. M. M. MORTLAND AND M. C. GASTUCHE, *C.R. Acad. Sci. Paris* **255,** 138 (1962).
18. H. P. KLUG AND L. E. ALEXANDER, "X-Ray Diffraction Procedures." Wiley, New York (1974).
19. M. C. GASTUCHE, G. BROWN, AND M. M. MORTLAND, *Clay Miner.* **7,** 177 (1967).
20. F. FREUND AND V. SPERLING, *Mater. Res. Bull.* **11,** 621 (1976).
21. W. FEITKNECHT AND H. W. BUSER, *Helv. Chim. Acta 34,* 128 (1951).
22. H. SCHÄFER AND F. WARTENPTUHL, *Z. Anorg. Chem.* **308,** 282 (1961).
23. F. FREUND, *J. Amer. Ceram. Soc.* **52,** 493 (1967).
24. C. C. ADDISON AND N. LOGAN, *Progr. Inorg. Chem. Radiochem.* **6,** 71 (1964).
25. C. C. ADDISON, J. LEWIS, AND R. THOMPSON, *J. Chem. Soc.,* 2829 (1951).
26. C. M. JOHNSON, M. G. SHILTON, AND A. T. HOWE, *J. Solid State Chem.* **37,** 37 (1981).
27. M. LAL AND A. T. HOWE, unpublished results.